Geolocation of North Sea cod (*Gadus morhua*) using hidden Markov models and behavioural switching

M.W. Pedersen, D. Righton, U.H. Thygesen, K.H. Andersen, and H. Madsen

Abstract: When geolocating fish based on archival tag data, a realistic assessment of uncertainty is essential. Here, we describe an application of a novel Fokker–Planck-based method to geolocate Atlantic cod (*Gadus morhua*) in the North Sea area. In this study, the geolocation relies mainly on matching tidal patterns in depth measurements when a fish spends a prolonged period of time at the seabed with a tidal database. Each day, the method provides a nonparametric probability distribution of the position of a tagged fish and therefore avoids enforcing a particular distribution, such as a Gaussian distribution. In addition to the tidal component of the geolocation, the model incoporates two behavioural states, either high or low activity, estimated directly from the depth data, that affect the diffusivity parameter of the model and improves the precision and realism of the geolocation significantly. The new method provides access to the probability distribution of the position of the fish that in turn provides a range of useful descriptive statistics, such as the path of the most probable movement. We compare the method with existing alternatives and discuss its potential in making population inference from archival tag data.

Résumé : Lorsqu'on fait la géolocalisation de poissons à partir de données provenant d'étiquettes à archivage, il est essentiel d'obtenir une évaluation réaliste de l'incertitude. Nous décrivons ici l'utilisation d'une méthode nouvelle basée sur l'équation de Fokker-Planck pour faire la géolocalisation des morues franches (*Gadus morhua*) dans la région de l'Atlantique Nord. Dans notre étude, la géolocalisation se base principalement sur l'appariement des patrons de marées dans les mesures de profondeur lorsqu'un poisson passe une période de temps prolongée sur le fond de la mer avec la banque de données sur les marées. Chaque jour, la méthode fournit une distribution non paramétrique de la position du poisson marqué et ainsi elle évite l'imposition d'une distribution particulière, par exemple la gaussienne. En plus de la composante tidale de la géolocalisation, le modèle incorpore deux états comportementaux, soit une activité forte et une activité faible, estimés directement à partir des données de profondeur, qui affectent le paramètre de diffusivité du modèle et améliorent significativement la précision et le réalisme de la géolocalisation. La nouvelle méthode donne accès à la distribution de probabilité de la position du poisson qui, à son tour, fournit une gamme de données statistiques descriptives utiles, telles que la piste la plus probable de déplacement. Nous comparons notre méthode avec les méthodes de rechange actuellement disponibles et discutons de son potentiel pour faire des déductions à partir de données provenant d'étiquettes à archivage.

[Traduit par la Rédaction]

Introduction

The application of advanced statistics when analysing data for tracking of marine animals has become increasingly popular during recent years. This trend is closely linked to the growing deployment of archival tags as data collectors attached to or within the tagged individual. Tags deliver highly accurate and oftentimes detailed information of the immediate environment of the host animal in the form of, e.g., depth, salinity, temperature, light, or oxygen content. These data can be used to estimate location of individuals, and so the introduction of electronic tags to the community of marine biology has spawned several geolocation studies. Heuristic methods vary in approach but typically focus on narrowing down the ensemble of possible locations by comparison of observations with outputs from environmental models (Metcalfe and Arnold 1997; Hunter et al. 2003; Neuenfeldt et al. 2007). The heuristic approaches to geolocation yield reasonable and at times accurate position estimates but do not fully exploit the autocorrelation of the observations, which, in turn, may limit the applicability of the methods when data quality is reduced.

Stochastic geolocation methods, i.e., methods assuming that the individual moves according to some stochastic process, have enabled the development of statistical tools to estimate horizontal movement of tagged fish and other animals (Nielsen 2004). The random walk process is prevalent within modelling of behavioural ecology (Okubo 1980) and has proven to be proficient in describing marine animal

Received 22 November 2007. Accepted 5 June 2008. Published on the NRC Research Press Web site at cjfas.nrc.ca on 15 October 2008.
J20280

M.W. Pedersen[1] and H. Madsen. Department for Informatics and Mathematical Modelling, Technical University of Denmark, 2800 Kgs. Lyngby, Denmark.
D. Righton. Centre for Environment, Fisheries and Aquaculture Science, Lowestoft Laboratory, Lowestoft, Suffolk NR33 0HT, UK.
U.H. Thygesen and K.H. Andersen. National Institute of Aquatic Resources, Technical University of Denmark, 2920 Charlottenlund, Denmark.

[1]Corresponding author (e-mail: mwp@imm.dtu.dk).

movements (Deriso et al. 1991; Sibert et al. 1999). Geolocation based on light measurements is commonly used for pelagic animals equipped with light-sensing tags (Welch and Eveson 1999) but suffers from excessive variation in latitude at periods of time close to the equinox (Musyl et al. 2001). To this end, the Kalman filter can be used to exploit the correlation of successive observations (Harvey 1989) and provide improved estimates of position. Furthermore, in assessing the uncertainty of each daily position estimate, the filter incorporates all observations to extract the maximum amount of information from the available data material (Sibert et al. 2003).

The Kalman filter relies on a Gaussian error assumption and therefore has the great advantage that it suffices to estimate the mean and variance of the position to describe the probability distribution on a given day. For geolocation of marine animals in the open ocean, the Kalman filter works well, but for fish moving close to shores, the parametric method is inadequate because it is likely to assign nonzero probability to dry land. A solution is the nonparametric particle filter method (Ristic et al. 2004), which simulates a large number of particles (fish) according to behavioural assumptions and environmental limitations, i.e., fish cannot move onto land, thereby avoiding the problem that the Kalman filter has. The framework has for geolocation purposes been applied to synthetic temperature measurements of the bluefin tuna (*Thunnus thynnus*) in the eastern Atlantic Ocean (Royer et al. 2005) and also Atlantic cod (*Gadus morhua*) in the Baltic Sea (Andersen et al. 2007). A drawback of the method is the enormous computational demands that arise owing to the number of particles that need to be simulated to obtain reliable parameter estimates (Andersen et al. 2007).

Methods of geolocation that are not based on light levels have yielded some of the longest time series of positional data to date (Hunter et al. 2005). Observations of wave patterns in depth records owing to tidal variations have proven to yield very accurate geolocations of, e.g., plaice (*Pleuronectes platessa*) (Metcalfe and Arnold 1997; Hunter et al. 2004), thornback ray (*Raja clavata*) (Hunter et al. 2005), and Atlantic cod (Righton et al. 2007; Gröger et al. 2007). These methods are based on a comparison of the observed tidal range and phase retrieved from the archival tag data with predictions from a tidal forecast model. Detection of a tidal pattern in the depth record from the tag implies an inactive fish dwelling at or very close to the seabed: the tag is thus recording the changing depth of the water column as the tide rises and falls over the fish. At other times, when fish are more active, tidal patterns are usually absent or difficult to detect with precision. Information about activity levels and changes in geographic location is fundamental to the analysis of behaviour modulation in demersal species (Righton et al. 2000) and greatly aids with objective classifications and interpretation of temporal and spatial differences in behaviour of individuals or populations (Hobson et al. 2007). It is at this point evident that, because cod and other demersal fish exhibit considerable seasonally dependent shifts in activity level (Turner et al. 2002), geolocating methods require greater sophistication to allow for time-varying changes in the behavioural state.

In the present study, we apply a direct Fokker–Planck-based methodology (FPM) using hidden Markov models to data from archival depth recorders attached to Atlantic cod in the North Sea (Pedersen 2007; Thygesen et al. 2008). The calculations were carried out on a laptop PC with the HMM geolocation toolbox (available from www.imm.dtu.dk/~mwp) for Matlab. Our aim was to obtain the most accurate recontruction of the geographic movements of cod and to describe these in terms of the estimated probability distribution of the position of the fish during its time at liberty and an estimate of the most likely route of migration. The geolocation method uses the detectable tidal patterns to partition the observed behaviour of the fish into two activity states, each with separate movement parameters that are estimated with the maximum likelihood method. Inferences on foraging–migration behaviour can then be made from the estimated parameter values, and the significance of the two-parameter model compared with the usual one-parameter model can be tested statistically in a likelihood ratio test. Using this method, we show that the uncertainty involved in fish tracking can be reduced considerably, enabling the fine-scale reconstruction of fish movements with a level of detail and information that could ultimately be used in behaviour-based models in fisheries assessment and management.

Materials and methods

In short, the geolocation technique applied here follows the principle of state–space modelling and Kalman filtering with time and data update steps but with the deviation that no assumptions are made about linearity or Gaussianity of the distribution of the states (Harvey 1989; Sibert et al. 2003; Patterson et al. 2008).

We assume that the fish performs a random walk in two-dimensional space with diffusivity D. We take the random walk to be isotropic (so that D is a scalar); we have no prior reason to believe that the fish should have a direction preference, so we elect to keep the model simple and leave the question of anisotropy to future studies. At time t, the fish has position $\boldsymbol{X}_t$ in two dimensions and we represent the estimate of this position explicitly by its probability density function $\phi(\boldsymbol{x}, t)$, a function of two-dimensional position $\boldsymbol{x} = (x_1, x_2)$ and time t. We discretize space on a quadratic grid over the North Sea; details will be given in the following section. In the filter, the time update propagates the probability density ϕ from the time of one measurement to the time of the next by solving the Fokker–Planck equation:

$$\frac{\partial \phi}{\partial t}(\boldsymbol{x}, t) = D\left[\frac{\partial^2 \phi}{\partial x_1^2}(\boldsymbol{x}, t) + \frac{\partial^2 \phi}{\partial x_2^2}(\boldsymbol{x}, t)\right]$$

This equation is solved numerically by finite-differences using the distribution at the previous time step as the initial condition. At time t of the next observation, some quantity $\boldsymbol{Y}$ is measured to have the value $\boldsymbol{y}$. In this paper, $\boldsymbol{Y}$ will typically be depth readings over the tidal cycle; details will be given in the following section. The filter then performs a data update using Bayes' formula to modify the probability distribution according to the information in the observation:

$$\phi(\boldsymbol{x}, t) \mapsto \frac{1}{\lambda_t}\phi(\boldsymbol{x}, t)\mathcal{L}(\boldsymbol{Y} = \boldsymbol{y}|\boldsymbol{X}_t = \boldsymbol{x})$$

Here, λ_t is a normalization constant, while $\mathcal{L}(\boldsymbol{Y} = \boldsymbol{y}|\boldsymbol{X}_t = \boldsymbol{x})$

Fig. 1. Example of archival tag data and illustration of the tidal and behaviour classification. (*a*) Depth record from tag No. 2255. (*b*) Part of the depth record for No. 2255 classified with respect to tidal information where the shaded regions mark the detected tidal patterns. (*c*) Depth record classified with respect to activity level, where shaded area denotes low activity level, and open area denotes high activity level. Note that the fish can have a high activity level although a tidal pattern is detected, e.g., around 24 October.

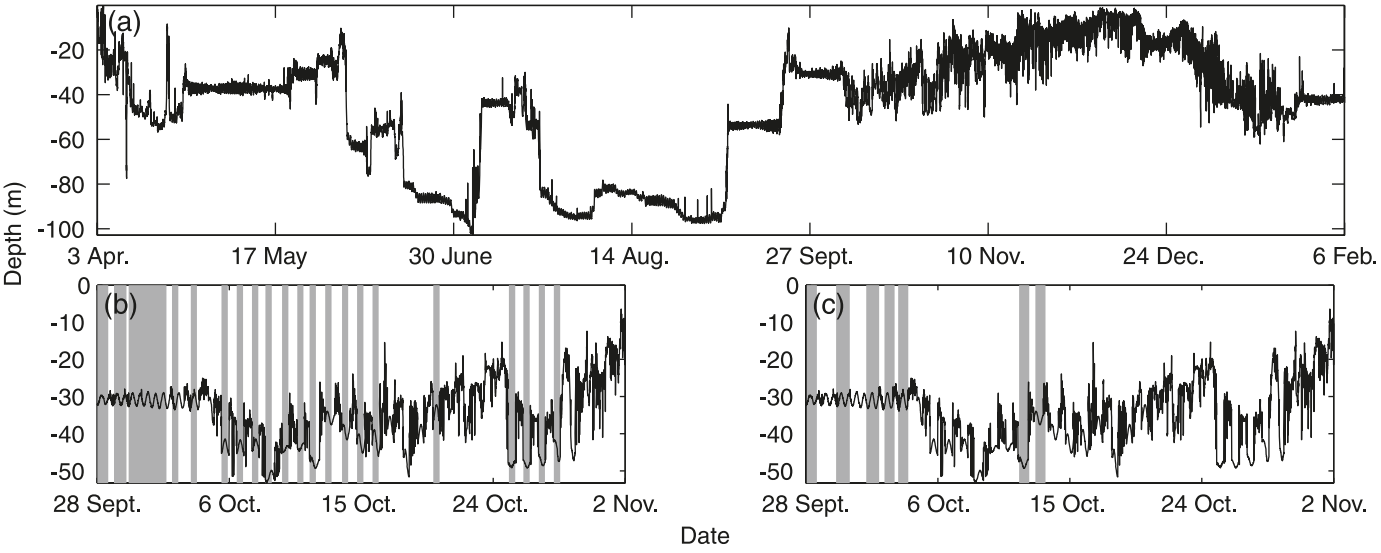

is termed the data likelihood and describes the probability of the observation for each possible position. We shall elaborate on this term in the following section.

The two update steps are run recursively in a manner analogous to the Kalman filter: first forward in time and then backward to smooth the estimates (Harvey 1989). The geolocations presented here rely on observations of depth and tide (Hunter et al. 2003) complemented by the release and recapture positions. The outcome of such a geolocation is the probability distribution of the position of the fish at all time steps throughout its time at liberty. For a mathematical walk-through of the method, the reader is referred to Pedersen (2007) and Thygesen et al. (2008). Given the probability distribution, it is possible to assess simply the most probable track that the fish took during its time at liberty, i.e., the mode of the joint distribution of all positions. To this end, the Viterbi algorithm (Viterbi 2006) is applied; this recursive algorithm provides the path through the states of a hidden Markov model that has the largest overall probability given the observations.

Data

The archival tags used to collect the data material for this study were of the type DST-Centi manufactured by Star-Oddi (www.star-oddi.com) and the slightly larger LTD 1200 manufactured by LOTEK (www.lotek.com). The resolution of depth measurements from the tags is approximately 0.05 m. The tags were programmed to record temperature and pressure (converted to depth upon download) every 10 min. The temperature records were not used in the present study. Fish to be tagged were caught by hook and line and anaesthetized before tagging to minimize the traumatization of the individual. The tagging procedure is described in greater detail in Righton et al. (2006). Data were retrieved from the tags after return through the commercial or recreational fishery.

The quantity and quality of tidal patterns in the resulting cod depth records show large variation between and within individuals. For example, the data record of cod No. 2255 (Fig. 1*a*) contains periods with smooth tidal patterns, periods with noisy tidal patterns, and periods without tidal patterns, making the tag well suited for the illustrative purpose of this paper. The cod was released on 3 April 2001 at 52.44°N, 1.78°E and recaptured 87 km away on 6 February 2002 at 52.00°N, 2.85°E, yielding a total time at liberty of 311 days. To show the versatility of the method, a less optimal data set from cod No. 1186 is also geolocated, which was released on 11 March 2005 at 50.3°N, 0.5°E and recaptured 395 km away on 19 January 2005 at 53°N, 4°E, yielding a total time at liberty of 315 days.

Tidal prediction model

The tides observed in the North Sea are mainly due to forcing from the Atlantic Ocean through the English Channel and north of the British Isles. At a particular location and time, the tide can be predicted by numerical forecast models. Such models split the tidal variation into a number of constituents that represent the characteristic modes of the system. A superposition of all modes yields the resulting wave that approximates the one observed in practice. For a constituent k, the depth variation $z_k(t, \boldsymbol{x})$ at a fixed position, $\boldsymbol{x}$, is fully represented by the function

$$(1) \qquad z_k(t, \boldsymbol{x}) = A_k(\boldsymbol{x}) \cos[\omega_k t - \theta_k(\boldsymbol{x}) + G_k]$$

where $A_k(\boldsymbol{x})$ and $\theta_k(\boldsymbol{x})$ are amplitude and phase, respectively, associated with this position $\boldsymbol{x}$, ω_k is the angular velocity, and G_k is the phase lag relative to time zero.

A forecast database from the Proudman Oceanographic Laboratory that included seven constituents (M2, S2, N2, K2, O1, K1, and M4) was used to predict tidal variations according to eq. 1. The database covers an area from 48°N to 60°N latitude and from 12°W to 8°E longitude with a reso-

Fig. 2. Amphidromic system of the North Sea here illustrated by the M2 constituent. The thick lines emanating from the amphidromic points are positions with a constant tidal phase relative to their numbering (hours). Intersecting perpendicular thin lines are positions with constant tidal range, i.e., difference between high water and low water in metres.

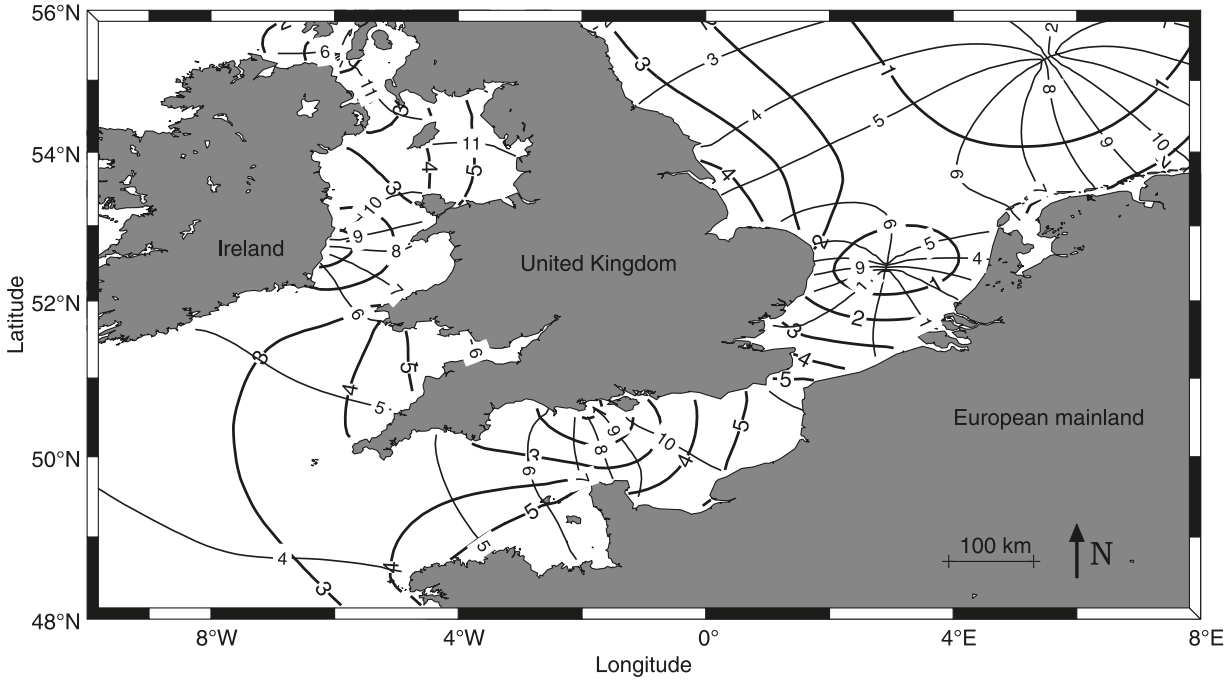

lution of 1/9° latitude and 1/6° longitude, approximately a 12 km × 12 km grid. The North Sea tidal system is roughly illustrated by observing its dominant constituent M2, which has a period of 12.42 h (Fig. 2).

Tidal extraction method

The observed time series was preprocessed to identify the time intervals in the depth record that contained a tidal pattern (Fig. 1). The extraction algorithm worked by sliding a 10 h window across the data and successively estimating the best least-squares fit of a sine function to the observations. The choice of window length is a trade-off: a shorter window length increases the number of successful fits but reduces the quality of each fit whereas a longer window length generates fewer fits but each with more statistical power. The window length of 10 h was chosen because it captures most of the dominant 12.4 h tidal cycle but also allows periods with tidal transport to be extracted. Of the 144 possible fits within each 24 h interval, the summary statistics root mean square error (rmse), R^2, and amplitude were extracted and the best fit (lowest rmse) was used as representative for this day. If the extracted summary statistics of the best fit fulfilled the criteria that rmse < 0.42 m, $R^2 > 0.85$, and amplitude > 0.6 m, the corresponding observed tidal pattern was stored for use in the data likelihood computation (see below). These limit values are hand-tuned parameters that were chosen so that the quality of extracted tidal signals was optimized. This tidal extraction technique bears strong resemblance to the methods applied in Hunter et al. (2003) and Gröger et al. (2007). If the criteria were not fulfilled, the maximum depth observation within the 24 h interval was stored to provide a means to confine the possible positions of the fish on the given day.

Behaviour classification

Previous studies have shown that the behaviour of cod tends to be divided into intervals of high and low activity (Righton et al. 2001). Modelling this dual-state behaviour with a single constant diffusivity would force the geolocation model to overestimate the uncertainty of the geolocation in some parts and underestimate it in other parts. In addition, if the different periods of high and low activity are not taken into account in the model, the diffusivity estimate for the entire data set will depend on the quality and type of the depth data and therefore make comparison of individuals difficult. As a partial solution to this, we extended the state–space of the system with a new state variable describing the activity level of the fish, thus making comparisons between individuals much less subjective.

The activity state is a time-dependent indicator function that, on a daily basis, is classified as either high or low. The state is, in principle, hidden (not directly observable), but to preserve the tractability of the problem, we estimated the activity state directly from the observed depth record before the actual geolocation step.

For each day in the time at liberty, the activity state of the fish is determined by testing the following hypotheses: H_0: the fish has a high level of activity (large value of diffusivity) and H_1: the fish has a low level of activity (small value of diffusivity). Only when H_0 is rejected at a sufficiently high level of significance can the small value of diffusivity be applied.

Following this thread, we construct a test to determine whether H_0 can be rejected. The test works in a way similar to the tidal extraction method by fitting a sine wave function to the observed depth in a 16 h sliding window rather than the 10 h window required for tidal data fitting. A fit con-

Fig. 3. Assumed autocorrelation contributions to the covariance structure of the observed 10 h tidal patterns: (*a*) white noise ($\mathbf{S}_E$); (*b*) autoregressive ($\mathbf{S}_\varepsilon$); (*c*) bathymetry uncertainty ($S_\eta(\boldsymbol{x})$); (*d*) tidal prediction uncertainty ($\mathbf{S}_e(\boldsymbol{x})$).

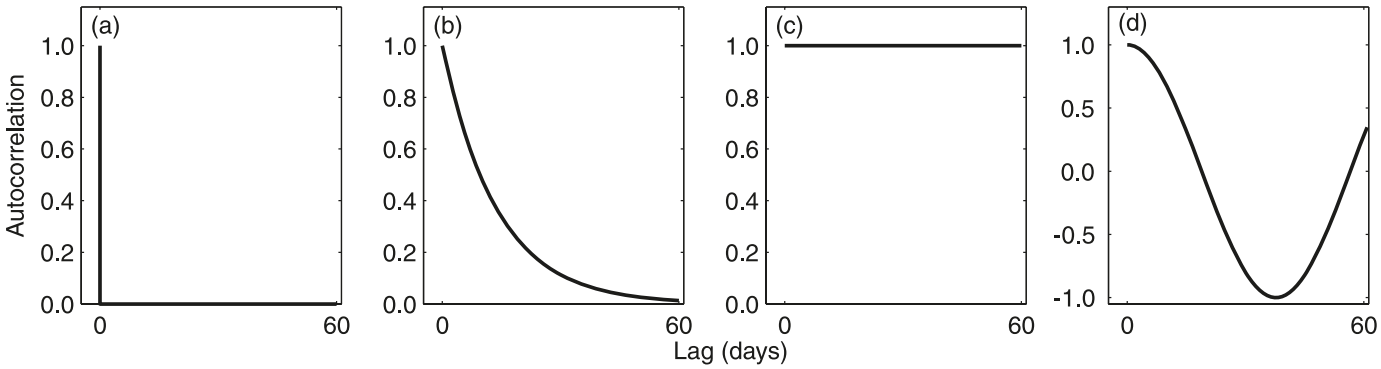

forming to the predefined limit values (see above) of rmse and R^2 rejects H_0 and implies a low level of activity in the current 24 h interval (Fig. 1). If H_0 cannot be rejected, a high level of activity is applied.

The algorithm relies on the assumption that a fish can only perform a limited migratory movement within a 24 h interval if it stays at the seabed for a continuous period of at least 16 h. Often, however, it is the case that the fish makes minor vertical excursions into the water column resulting in spikes in the tidal pattern. This makes the simple test fail, which in some cases will reject instances where a low activity would safely apply. To overcome this, the influence statistics of the 16 h fit are analysed to spot and exclude these outlying observations that deviate largely from the tidal pattern. This procedure greatly increases the detectable number of intervals with low activity within the time series and thus improves the uncertainty assessment.

Reconstructing the migration trajectory: building a data likelihood model

The data likelihood is a value computed for each position in the discrete grid describing the likelihood of the fish being in that position given the observation on the current day. The data likelihood is computed differently depending on the type of observation, i.e., it is computed either from the best extracted tidal pattern or from the maximum depth during that day if no tidal pattern was available.

Using the tidal pattern

The observed tidal pattern, denoted by the vector $\boldsymbol{Y}_j$ at day j, from a demersal fish consists of 60 depth observations (10 h fit sampled at a 10 min rate) and is assumed to follow a Gaussian distribution;

$$\boldsymbol{Y}_j \sim \mathcal{N}_{60}(\widehat{\boldsymbol{z}}_j(\boldsymbol{x}), \boldsymbol{\Sigma}(\boldsymbol{x}))$$

where $\widehat{\boldsymbol{z}}_j(\boldsymbol{x})$ is the predicted tidal pattern from the database at position $\boldsymbol{x}$ in the domain and $\boldsymbol{\Sigma}(\boldsymbol{x})$ is the covariance matrix that is a sum of four contributions:

$$\boldsymbol{\Sigma}(\boldsymbol{x}) = \mathbf{S}_E + \mathbf{S}_\varepsilon + S_\eta(\boldsymbol{x}) + \mathbf{S}_e(\boldsymbol{x})$$

where $\mathbf{S}_E$ has a white noise structure, $\mathbf{S}_\varepsilon$ has an autoregressive structure of first order, and $S_\eta(\boldsymbol{x})$ and $\mathbf{S}_e(\boldsymbol{x})$ are the uncertainty following the discretization of the domain for the bathymetry and tide, respectively (Fig. 3). The covariance matrices are estimated from the available data material prior to maximum likelihood estimation of the movement parameters (Pedersen 2007).

The white noise term (Fig. 3*a*) with a variance of $(0.2\ \text{m})^2$ describes the uncertainties invoked by the sensor resolution of the tag, by noise from environmental influences such as waves, and by other sources of error that are unknown and not explicitly modelled. The variance of the white noise was estimated by comparing observations from moored tags with the predicted tidal variations on the known location. In this way, the movement-related uncertainties were eliminated.

For a resident fish and a sample rate of 10 min, successive observations of depth will be correlated. Uncertainty owing to small-scale movements around rocks and holes in the seabed may therefore be modelled as an autoregressive process, $Y_i = \lambda Y_{i-1} + \varepsilon_i$ (Fig. 3*b*). As the statistical estimation of the parameter values, λ and the variance of ε_i, is not immediately feasible, we used heuristic estimates based on the assumption that the small-scale movement of the fish has decorrelated (reached an autocorrelation of <0.05) after 7 h. This results in $\lambda = 0.93$. For minor depth variations owing to small-scale movement, we conservatively set the variance of ε_i equal to $(0.4\ \text{m})^2$. More work is required to analyse the small-scale movements to confirm these assumptions, but the spatiotemporal dependence of fish movements makes this exercise complex and is best supported by more sophisticated observations, e.g., from an accelerometer; this study is beyond the scope of this paper.

A bottom-dwelling fish is likely to record a mean depth several metres off the prediction of the bathymetry when positioned in an area with a large depth gradient. This bathymetry uncertainty is estimated by comparing the depth of each grid cell with the maximal depth of its neighbouring grid cells. The estimated bathymetry variance, $S_\eta(\boldsymbol{x})$, accounts for the large-scale variation by adding a spatial-dependent but time-constant variance to the observations (Fig. 3*c*) in the range from $\sim 0\ \text{m}^2$ to $(750\ \text{m})^2$. A large value of the bathymetry variance means that the confidence of the observed depth level is reduced and hence that the geolocation at this position relies only on the tidal pattern if one is available. Analogous to the bathymetry variance, uncertainty in the tidal predictions is imposed owing to the spatial discretisation. The difference within a grid cell between tidal predictions of two distinct positions will

Fig. 4. Principle of the data likelihood computation when a tidal pattern is present. (*a*) Observed depth compared with the corresponding predictions from the tidal model at three distinct positions marked in Fig. 4*b*. (*b*) The light grey areas are the 95% confidence areas for the data likelihood. It is evident that multiple predictions fit the observed tidal signal because of the ambiguous nature of the amphidromic system. In this particular example, locations 1 and 2 fit well with the observed signal, whereas location 3 clearly does not.

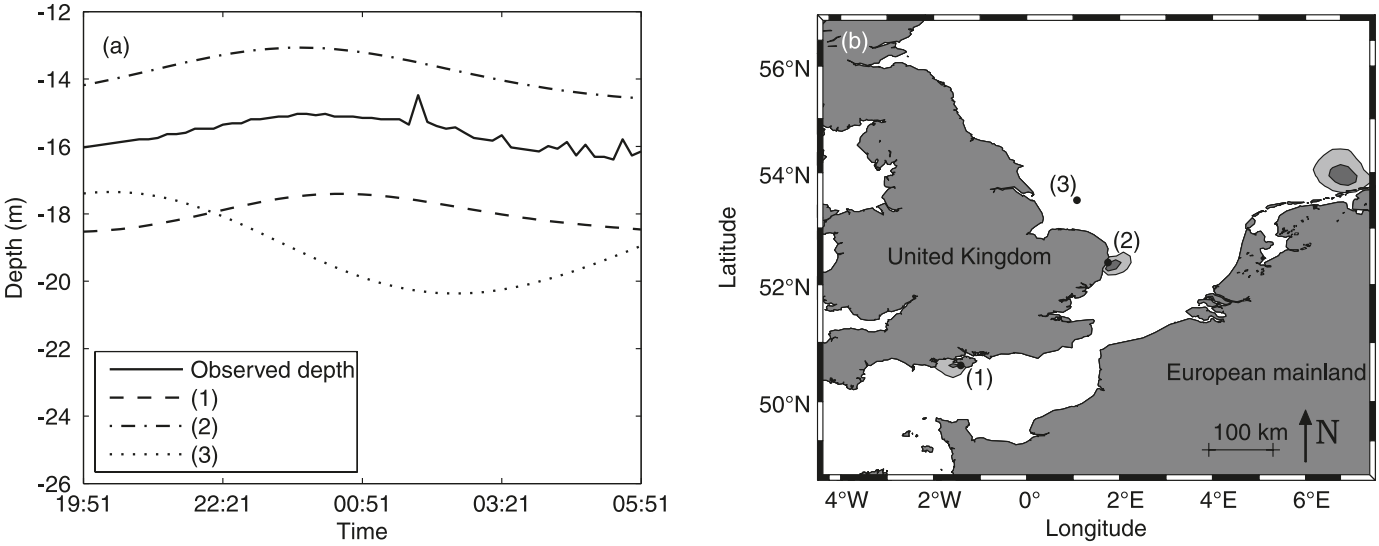

show a sinusiodal waveform because of slight differences in amplitude and phase (Fig. 3*d*). This is accounted for by computing the variance of the tidal prediction, $\mathbf{S}_e(\boldsymbol{x})$, and including this in $\boldsymbol{\Sigma}(\boldsymbol{x})$. The tidal prediction uncertainty is computed by comparing neighbouring cells in a way similar to the bathymetry uncertainty. The range of $\mathbf{S}_e(\boldsymbol{x})$ is from ~ 0 m^2 to (0.97 m)^2.

The result of a data likelihood computation is an array of size equal to the discrete domain containing the likelihood of each position given the observed data (Fig. 4). Owing to the ambiguity of the amphidromic system, multiple positions typically appear equally likely although they are spatially separated. The statistical filter (Thygesen et al. 2008) and in particular the smoothing step will remove most of this multimodality by conditioning the resulting estimated probability distribution on future as well as past observations within the time at liberty.

The data likelihood at position $\boldsymbol{x}$ is written formally as

$$\mathcal{L}(\boldsymbol{Y}_j = \boldsymbol{y}_j | \boldsymbol{X} = \boldsymbol{x}) = \frac{1}{(2\pi)^{30}\sqrt{\det\,\boldsymbol{\Sigma}(\boldsymbol{x})}} \times \exp\left\{-\frac{1}{2}\left[\boldsymbol{y}_j - \hat{\boldsymbol{z}}_j(\boldsymbol{x})\right]^T \boldsymbol{\Sigma}(\boldsymbol{x})^{-1}\left[\boldsymbol{y}_j - \hat{\boldsymbol{z}}_j(\boldsymbol{x})\right]\right\}$$

i.e., the probability density function of a 60-dimensional Gaussian distribution.

Using the maximum depth

In the absence of a tidal pattern in the observations on a given, day there remains valuable information in the depth record that can be used for geolocation. Previous studies have simply excluded positions shallower than the maximum observed depth in the tag within some uncertainty bounds (Ådlandsvik et al. 2007). Instead of a threshold, we assign in the data likelihood a value between 0 and 1 to each position dependent on its depth and bathymetry variance compared with the observed depth. This provides a more informative data likelihood than the simple indicator and exploits the important information in the bathymetry variance. This is of particular importance, as the variance of the bathymetry strongly depends on the position in that the depth of a grid cell on a slope has a high variance compared with the depth of a grid cell in a flat area.

The data likelihood computation method, inspired by the one applied in Andersen et al. (2007), assumes that the observed depth at a given position is Gaussian distributed with mean equal to the depth of the bathymetry, $z(\boldsymbol{x})$, and variance equal to the estimated bathymetry variance, $S_\eta(\boldsymbol{x})$. The likelihood of a position given a maximum observed depth (Fig. 5), $\overline{z}_j$, is found by

$$\mathcal{L}(\boldsymbol{Y}_j = \boldsymbol{y}_j | \boldsymbol{X} = \boldsymbol{x}) = \Phi\left[\frac{\overline{z}_j - z(\boldsymbol{x})}{\sqrt{S_\eta(\boldsymbol{x})}}\right] \Phi\left[\frac{-z(\boldsymbol{x})}{\sqrt{S_\eta(\boldsymbol{x})}}\right]^{-1} \quad (2)$$

where Φ is defined as the cumulated density function of a standardized Gaussian distribution with the constraint (truncation) $\overline{z}_j < 0$ and $z(\boldsymbol{x}) < 0$; hence, the normalization, at $\overline{z}_j = 0$, in eq. 2 is required because we cannot observe positive depths, and therefore, an observed depth of >0 m must always result in a data likelihood value of 1.

Supplementing with the recapture position

Typically, a recapture position is reported at the retrieval of the tag. This position may be subject to misreporting or inaccuracy. Regardless, the recapture position is of particular importance if tidal information is scarce and will effectively rule out dead ends and narrow down the estimated probability distribution towards the end of the time at liberty.

We modelled the reported recapture position as an unbiased measurement, where the error is bivariate Gaussian. We chose the variance in this distribution subjectively but conservatively. The choice of a Gaussian distribution is purely arbitrary owing to a lack of information about this

Fig. 5. Principle of the data likelihood computation when a tidal pattern is absent. (*a*) The maximum depth within the 24 h interval is used when a tidal pattern is undetectable. (*b*) Data likelihood computation for a candidate position. To determine the likelihood value, the maximum observed depth value is compared with a truncated Gaussian cumulated density function with mean and variance equal to the depth and bathymetry variance at the given position.

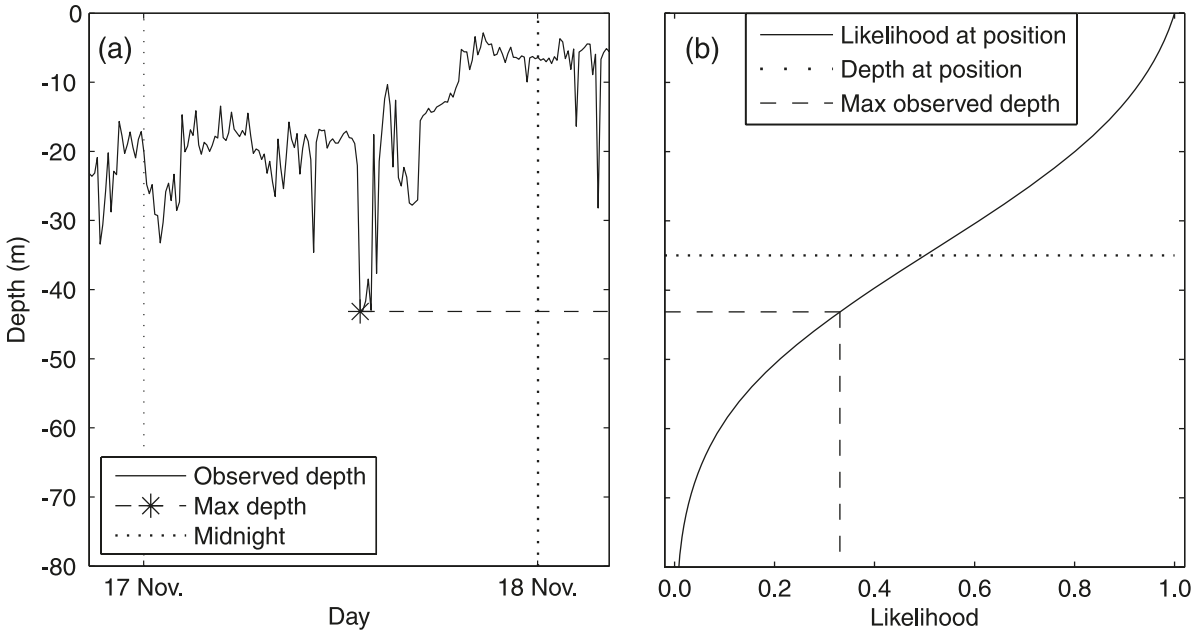

Fig. 6. Most probable track of tag No. 2255; the solid circle is the initial position of partial track and the shaded circle is the end position of the partial track. (*a*) The fish was released off Lowestoft on 3 April and migrated north to its summer residence by 30 April. (*b*) Here, it stayed until 18 November and performed only minor swimming activity during this period. (*c*) Then the fish returned to the southern North Sea and was recaptured close to the English channel on 6 February of the following year.

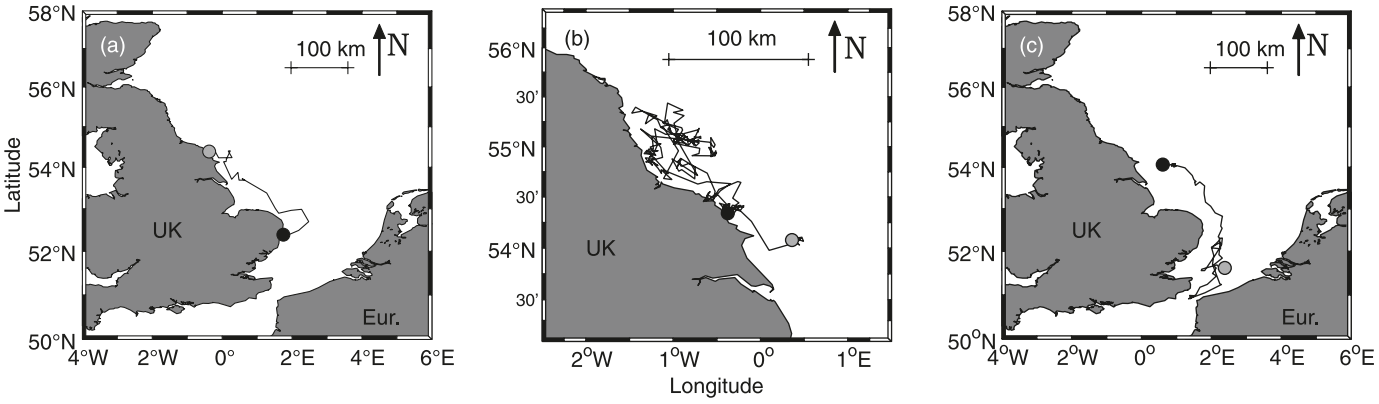

distribution. One might in some cases consider applying a *t* distribution with a small number of degrees of freedom to increase the probability of extreme deviations between the actual and the reported recapture.

By conditioning on the position, the depth observations and the reported recapture position become independent stochastic variables. Therefore, the likelihood contributions from the two terms are simply multiplied to obtain the data likelihood function.

Results

Tag No. 2255

The cod was captured, tagged, and released close to Lowestoft, UK, and, according to the most probable track, immediately began a migration to the north, settling down after a month at approximately 54.5°N, 0.5°W (Fig. 6*a*). Here, it stayed for another month before relocating a bit farther north to an area around 55°N, 1°W, where it stayed for a prolonged period until late September at a constant depth of around 90 m (Fig. 6*b*). Then the activity level gradually increased and eventually a southwards migration brought the cod to a position at 51.75°N, 2.5°E, around 9 January and was recaptured a month later at approximately this position (Fig. 6*c*). The cod showed many long periods of inactivity, particularly during the summer when a continuous smooth tidal signal was measured spanning more than a month from late July until early September. The tidal extraction al-

Fig. 7. Probability distributions of the position of tag No. 2255 on (*a*) 23 June 2001 and (*b*) 6 December 2001 estimated in the two-mode behaviour model. Light shading is the 95% confidence region, dark shading is the 50% confidence region, and the circle is the mode of the distribution. (*a*) The distribution off the northern English coast is narrow owing to the high quality of tidal information and low activity mode of the fish in this time step. (*b*) Distribution at a time step where the fish was pelagic, i.e., no observed tidal information, thus causing the distribution to widen. The maximum recorded depth is used to exclude positions on the Dogger Bank, enforcing a hole in the distribution. This illustrates the ability of the method to estimate distributions that take on arbitrary forms.

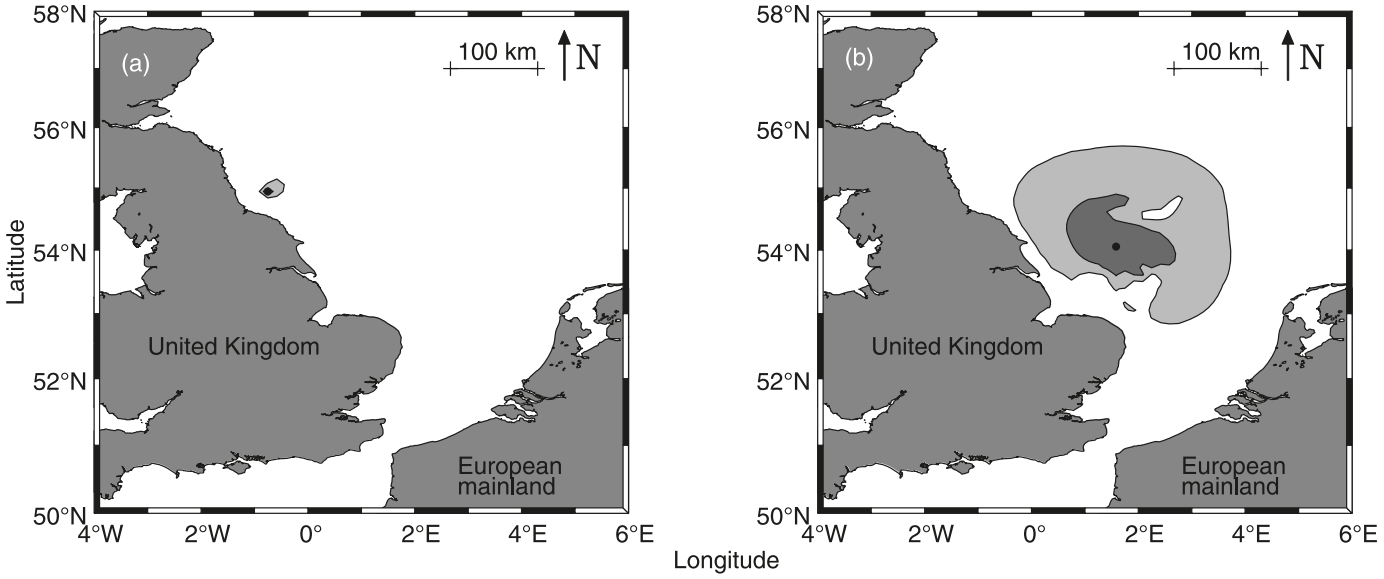

gorithm found a total of 198 days with a tidal pattern of sufficient quality out of the 311 days that the fish was at liberty.

The maximum likelihood estimates (MLEs) of the diffusivities were 17.4 and 149 km^2·day^{-1} for low and high activity, respectively, with a standard deviation of 2.69 and 28.5 km^2·day^{-1}, respectively. The MLEs were found using the simplex search method. The likelihood surface was smooth around the optima, which enabled us to estimate the uncertainty of the MLEs from the Fisher information. For comparison, we carried out a calculation with only one movement parameter, i.e., one behavioural state. This resulted in a MLE of the diffusivity of 57.6 km^2·day^{-1} with a standard deviation of 6.6 km^2·day^{-1}. The statistical difference of the two parameterizations can be quantified by a likelihood ratio test. This essentially determines if a two-diffusivity model improves the likelihood of the MLE significantly compared with a one-diffusivity model, i.e., it determines whether the fish showed at least two different types of behaviour. The likelihood ratio test statistic is $Z_{\mathrm{LR}} = 2[\ell(\widehat{D}) - \ell(\widehat{D}_0)] = 68$, where $\ell(\widehat{D}_0)$ is the log-likelihood value of the MLE in the one-diffusivity case, and $\ell(\widehat{D})$ is the log-likelihood value of the MLE in the two-diffusivity case. The test statistic Z_{LR} is χ^2 distributed with 1 degree of freedom resulting in a p value for the test of $p < 10^{-15}$, which is highly significant at all reasonable levels. This result provides evidence that No. 2255 switches its activity level in a way that is well estimated by the classification algorithm.

The uncertainty of the marginal distributions estimated on a daily basis depends on the diffusivity estimate and on the type and quality of data. At times, particularly in the first half of the data set when the activity level was low, the marginal distributions were very narrow (Fig. 7*a*). Often, in this period, the precision of the geolocation was limited by the discretisation (12 km × 12 km) of the domain rather than of the quality of the data. In the latter part of the data set where activity was high, the estimated marginal distributions widened owing to the lack of tidal information in the depth record (Fig. 7*b*), an unavoidable uncertainty of the position given the low quality of the information available.

Access to the probability distribution of the position allows us to sample random outcomes of this distribution, i.e., random tracks that the fish might have swum. By sampling of a batch of tracks, we can estimate the probability of the fish having visited some specific region, e.g., crossed the border of a marine protected area or the probability of the fish having picked one of many possible routes to reach a destination (Ådlandsvik et al. 2007, their figure 5*b*). Here, we sampled 1000 random paths of tag No. 2255 and found that 54 of the random paths entered ICES area VIId in the eastern English Channel towards the end of its time at liberty. Crudely, this equates to a 5.4% probability of this event, although a more robust statistical framework would be required to evaluate the significance of this result in a fisheries management context. Nonetheless, it is an indication that summary statistics of this type may be relevant to estimate if one wishes to investigate the mixing of populations and the behaviour of individuals in relation, e.g., to ICES areas.

Tag No. 1186

The estimated movement of this cod shows a similar type of periodicity as tag No. 2255 (Fig. 8). The fish was at liberty for 315 days and spent its first 3 months migrating west from its release position in the eastern English Channel (Fig. 8*a*). For 6 months, it resided at the western end of the English Channel in the Celtic Sea (Fig. 8*b*) before returning

Fig. 8. Most probable track of tag No. 1186; the solid circle is the initial position of partial track and the shaded circle is the end position of the partial track. (*a*) The fish was released in the eastern English Channel on 11 March and migrated west through the Hurd Deep area over a period of 3 months. (*b*) From 1 June to 5 December, it stayed just west of the English Channel within a relatively limited area. (*c*) Then it executed a migration east through the English Channel and into the southern North Sea in a time span of just over a month, being recaptured eventually on 19 January of the following year.

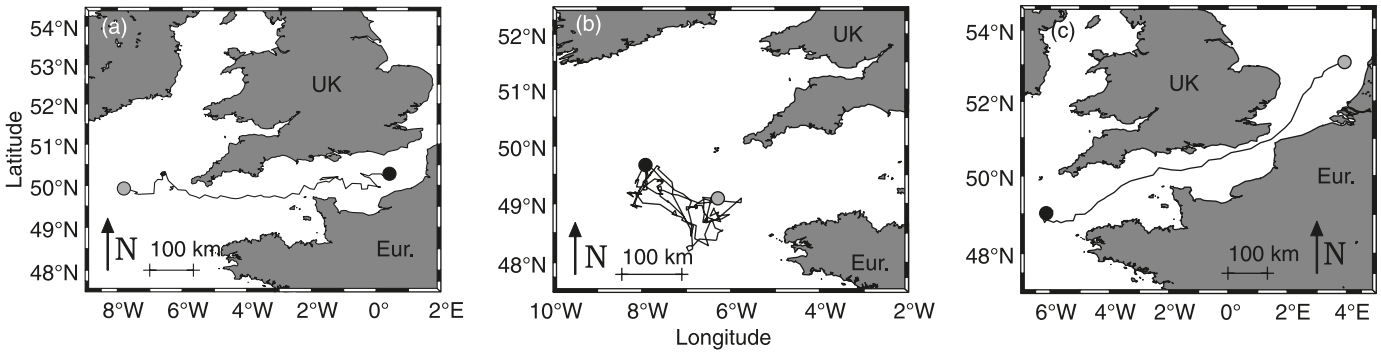

east and continuing the migration to the southern North Sea (Fig. 8*c*).

The movement away from the English Channel into the Atlantic Ocean where tidal variation is less pronounced resulted in high values of the diffusivity estimates and with large variance. In such a case of reduced data quality, it may be reasonable to use, as prior information, the diffusivity estimates from a high-quality depth record (such as No. 2255) geolocated in areas with prominent tidal variation to improve the geolocation. Without applying this correction, the apparent movement in the residing period (Fig. 8*b*) may be due to uncertainty in the tidal forecast model. To correct for this, it would be required to also consult the estimated probability distribution that expresses the geolocation uncertainty.

Again, the nature of the track with clear periods of high and low activity emphasizes the need for at least two regimes in the behaviour model. This matter is well illustrated by the return migration where a distance of 900 km is covered in 41 days as compared with the much lower activity in the middle part of the time at liberty.

Discussion

The geolocation method that we have described, termed a direct FPM, is a considerable evolution of the tidal geolocation method (TLM) described in Hunter et al. (2003). We made two fundamental advances: (*i*) successive geolocations, even those separated by many days, were linked together to create a continuous estimate of geographic location, and (*ii*) correlation of position estimates was implemented rather than treating singular positions as independent observations. This has the benefit that not only are reconstructions of migrations more precise, the reconstructions provide a genuine assessment of certainty that a sequence of independently reconstructed geographic locations can sometimes falsely convey. In addition to these advances, our method achieved greater accuracy of geolocation by taking the behaviour of individuals into account.

Accuracy of the FPM

Errors in the FPM can occur at one or more of the stages of the reconstruction process, and a considerable advantage of the method is that most of these errors can either be controlled or reported on so that an integrated assessment of the reliability of the migration reconstructions can be made. The errors that are most likely to occur are estimation of tidal parameters in the data record, error in the tidal database itself (Hunter et al. 2003), estimation of the (two different) diffusion coefficients, and error during the filtering process (Thygesen et al. 2008). For example, the mean positional error of the TLM varies between 10 and 80 km, depending on location, with the greatest errors found at locations midway between amphidromic points.

Overall, however, the errors generated by estimating tidal parameters and the uncertainty that can arise when suitable tidal data cannot be extracted are likely to be the greatest source of uncertainty in reconstructing migration pathways (Hunter et al. 2003), i.e., fish spend only brief periods of time close to the seabed and are highly mobile at other times (Hunter et al. 2006; Righton et al. 2007). In the absence of a tidal pattern, the FPM only uses the maximum depth on the given day to give some coarse geolocation. The FPM therefore addresses the problem of low information implicitly by using what knowledge that can be extracted from the depth record, and the information on prior and succeeding geolocations, to adjust the uncertainty of the geolocations. The geolocation of a given day is therefore conditioned on the information of all days and uncertainty is reduced even when the data information on the specific day is weak.

The FPM also addresses the problem that animals tend to move in irregular patterns with many small movements interspersed with the occasional large movement (Benhamou 2007; Sims et al. 2008). Our method, if necessary, derives two diffusivity values related to different activity levels of the fish to directly adjust the uncertainty of geolocation at different times. At other times, if the observations do not imply that the fish has two behaviours, the maximum likelihood estimate of the two diffusivity parameters is reduced to one diffusivity parameter. Our results show that this method is statistically robust and provides a more accurate measure of position on any given day than by using a single parameter. The model also shows that multiple activity levels are a feature of cod behaviour and migration. For data sets in which the distinction between different behaviours is less

obvious, it should still be possible to include and estimate the activity level as a hidden state within the hidden Markov model filter. However, this approach complicates matters significantly in terms of statistical implementation and computational demands and is far from a trivial task. Additionally, in theory, there is no reason why the model could not be extended to include several more levels of activity at the expense of run time, although it would not be likely to add much more information than the two-parameter model currently provides and may be very difficult to parameterize and validate. As it is, the model is already capable of providing a much more accurate and precise estimate of location and movement rate than was previously possible.

Ultimately, it is not trivial to give a single standardized measure of the accuracy of the FPM in reconstructing the migrations of cod because of the lack of data against which to validate the positional estimates. Initial studies showed that geolocation analyses of moored tags yielded consistent position estimates that were in correspondence to their true geographical position (Pedersen 2007). In this sense, the FPM produces accurate results, even though temperature data were not used to validate positional estimates. In addition, the method also produces qualitatively similar results to reconstructions made with a simulation method (Righton and Mills 2008) that uses depth and temperature data to estimate geoposition and therefore successfully captures the same overall pattern of movements of individual cod, as have been described previously (Turner et al. 2002; Righton et al. 2007). However, the relative simplicity (depth only) and transparency of the FPM gives it an advantage over the simulation method because it requires only bathymetry and a tidal database rather than a temporally and spatially resolved temperature database.

Application of the FPM

The TLM has been used to describe the migrations of plaice in the North Sea (Hunter et al. 2004), but the application of the method to other species has been limited because few other species that are large enough to be fitted with electronic tags spend sufficient time close enough to the seafloor for similar analyses to be undertaken. In addition, the TLM can be time intensive and produce multiple estimates of location that can be difficult to discriminate between. Together, these problems can hamper the reconstruction of migration pathways in cod (or any species that spends significant time away from the seabed) because suitable algorithms for processing the uncertainty have not, until now, been available (Turner et al. 2002; Hunter et al. 2003). Reconstructions of migrations of, e.g., cod to date have therefore been necessarily simplistic (Righton et al. 2007). Our reconstructions of cod migrations with the FPM showed that, even though there may be long periods of time when individuals cannot be located using the TLM, the inferential power of the FPM provides valuable daily estimates of position and the uncertainty of those estimates. The quality and frequency of the positional estimates are sufficient enough that it is easy to imagine their use within individual-based models of fish movement, therefore enabling simulations of the effect of stock movements or mixing. The nonparametric representation of the estimated probability distribution also makes the FPM a source for interesting new applications of archival tag data. The ability of the method to handle any type of archival tag data and a free choice of data likelihood computation technique can make the FPM a building block for more advanced statistical geolocation such as implementation of complex behaviour models or incorporation of robustness towards outlying position estimates, e.g., from GPS tags or from light-based tags that provide raw geolocations as output. In turn, these advances make possible new analyses of migration mechanisms and behaviours and will help to shed light on the underlying behavioural processes that govern habitat selection or foraging behaviour (Sims et al. 2006).

Models of population movement used to delineate the structure of fish stocks or changes in abundance in space and time are becoming increasingly sophisticated (Metcalfe 2006; Metcalfe et al. 2008). This has been encouraged by the requirement for "evidence-based" fisheries policies. A recurring theme of these policies, considering the difficulty of characterizing accurately the features of the marine environment, is the need for assessments of how reliable the information is and to attach an estimate of certainty to any evidence that may be used to define or support policies. At a basic level, estimating the likelihood that an individual visits a delineated area is an important first step because this has an immediate application to identifying stock identity and the risk of capture as well as to the potential utility of closed areas. A direct link to population-level models has yet to be developed for the FPM method, but a crude approach that simply averages multiple distribution estimates could be used as a first approach (Andersen et al. 2007). However, high-quality representative data sets are needed to create a statistical population model with a large number (>100) of reconstructed migrations that capture the appropriate spatial and temporal scales (Hunter et al. 2005). This applies not only at the individual level but also with respect to the experimental design of the tagging study, i.e., data spanning all seasons and possibly stratified spatially as well as with respect to age and species. One should therefore bear in mind the application of geolocation techniques when planning new studies and enhancing existing studies.

References

Andersen, K.H., Nielsen, A., Thygesen, U.H., Hinrichsen, H.H., and Neuenfeldt, S. 2007. Using the particle filter to geolocate Atlantic cod (*Gadus morhua*) in the Baltic Sea, with special emphasis on determining uncertainty. Can. J. Fish. Aquat. Sci. **64**: 618–627. doi:10.1139/F07-037.

Ådlandsvik, B., Huse, G., and Michaelsen, K. 2007. Introducing a method for extracting horizontal migration patters from data storage tags. Hydrobiologia, **582**: 187–197. doi:10.1007/s10750-006-0556-7.

Benhamou, S. 2007. How many animals really do the Lévy walk? Ecology, **88**: 1962–1969. doi:10.1890/06-1769.1. PMID: 17824427.

Deriso, R.B., Punsly, R.G., and Bayliff, W.H. 1991. A Markov movement model of yellowfin tuna in the eastern Pacific Ocean and some analyses for international management. Fish. Res. **11**: 375–395. doi:10.1016/0165-7836(91)90010-D.

Gröger, J.P., Rountree, R.A., Thygesen, U.H., Jones, D., Martins, D., Xu, Q., and Rothschild, B.J. 2007. Geolocation of Atlantic cod (*Gadus morhua*) movements in the Gulf of Maine using tidal information. Fish. Oceanogr. **16**: 317–335. doi:10.1111/j.1365-2419.2007.00433.x.

Harvey, A.C. 1989. Forecasting, structural time series models and the Kalman filter. Cambridge University Press, London.

Hobson, V.J., Righton, D., Metcalfe, J.D., and Hays, G.C. 2007. Vertical movements of North Sea cod. Mar. Ecol. Prog. Ser. **347**: 101–110. doi:10.3354/meps07047.

Hunter, E., Aldridge, J.N., Metcalfe, J.D., and Arnold, G.P. 2003. Geolocation of free-ranging fish on the European continental shelf as determined from environmental variables. Mar. Biol. (Berl.), **142**: 601–609.

Hunter, E., Metcalfe, J.D., Holford, B.H., and Arnold, G.P. 2004. Geolocation of free-ranging fish on the European continental shelf as determined from environmental variables II. Reconstruction of plaice ground tracks. Mar. Biol. (Berl.), **144**: 787–798. doi:10.1007/s00227-003-1242-1.

Hunter, E., Buckley, A.A., Stewart, C., and Metcalfe, J.D. 2005. Migratory behaviour of the thornback ray, *Raja clavata*, in the southern North Sea. J. Mar. Biol. Assoc. U.K. **85**: 1095–1105. doi:10.1017/S0025315405012142.

Hunter, E., Berry, F., Buckley, A., Stewart, C., and Metcalfe, J. 2006. Seasonal migration of thornback rays and implications for closure management. J. Appl. Ecol. **43**: 710–720. doi:10.1111/j.1365-2664.2006.01194.x.

Metcalfe, J. 2006. Fish population structuring in the North Sea: understanding processes and mechanisms from studies of the movements of adults. J. Fish Biol. **69**: 48–65. doi:10.1111/j.1095-8649.2006.01275.x.

Metcalfe, J.D., and Arnold, G.P. 1997. Tracking fish with electronic tags. Nature (London), **387**: 665–666. doi:10.1038/42622.

Metcalfe, J.D., Righton, D.A., Hunter, E., and Eastwood, P. 2008. Migration and habitat choice in marine fishes. *In* Fish behaviour. *Edited by* C. Magnhagen, V.A. Braithwaite, E. Forsgren, and B.G. Kapoor. Science Publishers Inc., Enfield, N.H.

Musyl, M.K., Brill, R.W., Curran, D.S., Gunn, J.S., Hartog, J.R., Hill, R.D., Welch, D.W., Eveson, J.P., Boggs, C.H., and Brainard, R.E. 2001. Ability of archival tags to provide estimates of geographical position based on light intensity. *In* Electronic tagging and tracking in marine fisheries reviews: methods and technologies in fish biology and fisheries. *Edited by* J. Sibert and J. Nielsen. Kluwer Academic Press, Dordrecht, the Netherlands. pp. 343–368.

Neuenfeldt, S., Hinrichsen, H.H., Nielsen, A., and Andersen, K.H. 2007. Reconstructing migrations of individual cod (*Gadus morhua* L.) in the Baltic Sea by using electronic data storage tags. Fish. Oceanogr. **16**: 526–535. doi:10.1111/j.1365-2419.2007.00458.x.

Nielsen, A. 2004. Estimating fish movement. Ph.D. thesis, Royal Veterinary and Agricultural University, Copenhagen, Denmark.

Okubo, A. 1980. Diffusion and ecological problems: mathematical models. Springer-Verlag, New York.

Patterson, T., Thomas, L., Wilcox, C., Ovaskainen, O., and Matthiopoulos, J. 2008. State–space models of individual animal movement. Trends Ecol. Evol. **23**: 87–94. doi:10.1016/j.tree.2007.10.009. PMID:18191283.

Pedersen, M.W. 2007. Hidden Markov models for geolocation of fish. M.Sc. thesis, Informatics and Mathematical Modelling, Technical University of Denmark, DTU, Kgs. Lyngby, Denmark. IMM Publication.

Righton, D., and Mills, C. 2008. Reconstructing the movements of free-ranging demersal fish in the North Sea: a data-matching and simulation method. Mar. Biol. (Berl.), **153**: 507–521. doi:10.1007/s00227-007-0818-6.

Righton, D., Turner, K., and Metcalfe, J.D. 2000. Behavioural switching in North Sea cod: implications for foraging strategy? ICES CM Q:09.

Righton, D., Metcalfe, J.D., and Connolly, P. 2001. Different behaviour of North and Irish Sea cod. Nature (London), **411**: 156. doi:10.1038/35075667.

Righton, D., Kjesbu, O.S., and Metcalfe, J.D. 2006. A field and experimental evaluation of the effect of data storage tags on the growth of cod. J. Fish Biol. **68**: 385–400. doi:10.1111/j.0022-1112.2006.00899.x.

Righton, D., Quayle, V., Hetherington, S., and Burt, G. 2007. Movements and distribution of cod (*Gadus morhua* L.) in the southern North Sea and English Channel: results from conventional and electronic tagging experiments. J. Mar. Biol. Assoc. U.K. **87**: 599–613. doi:10.1017/S0025315407054641.

Ristic, B., Arulampalam, S., and Gordon, N. 2004. Beyond the Kalman filter. Particle filters for tracking applications. Artech House Publishers, Boston, Mass.

Royer, F., Fromentin, J.-M., and Gaspar, P. 2005. A state–space model to derive bluefin tuna movement and habitat from archival tags. Oikos, **109**: 473–484. doi:10.1111/j.0030-1299.2005.13777.x.

Sibert, J.R., Hampton, J., Fournier, D.A., and Bills, P.J. 1999. An advection–diffusion–reaction model for the estimation of fish movement parameters from tagging data, with application to skipjack tuna (*Katsuwonus pelamis*). Can. J. Fish. Aquat. Sci. **56**: 925–938. doi:10.1139/cjfas-56-6-925.

Sibert, J.R., Musyl, M.K., and Brill, R.W. 2003. Horizontal movements of bigeye tuna (*Thunnus obesus*) near Hawaii determined by Kalman filter analysis of archival tagging data. Fish. Oceanogr. **12**: 141–151. doi:10.1046/j.1365-2419.2003.00228.x.

Sims, D., Witt, M., Richardson, A., Southall, E., and Metcalfe, J. 2006. Encounter success of free-ranging marine predator movements across a dynamic prey landscape. Proc. R. Soc. Lond. Ser. B Biol. Sci. **273**: 1195–1201. doi:10.1098/rspb.2005.3444.

Sims, D.W., Southall, E.J., Humphries, N.E., Hays, G.C., Bradshaw, C.J.A., Pitchford, J.W., James, A., Ahmed, M.Z., Brierley, A.S., Hindell, M.A., Morritt, D., Musy, M.K., Righton, D., Shepard, E.L.C.Wearmouth, V.J., Wilson, R.P., Witt, M.J., and Metcalfe, J.D. 2008. Scaling laws of marine predator search behaviour. Nature (London), **451**: 1098–1102. doi:10.1038/nature06518. PMID:18305542.

Thygesen, U.H., Pedersen, M.W., and Madsen, H. 2008. Geolocating fish using hidden Markov models and data storage tags. *In* Tagging and tracking of marine animals with electronic devices II. Volume 8 reviews: methods and technologies in fish biology and fisheries. *Edited by* J.L. Nielsen, H. Arrizabalaga, N. Fragoso, A. Hobday, M. Lutcavage, and J. Sibert. Springer, The Netherlands. In press.

Turner, K., Righton, D., and Metcalfe, J.D. 2002. The dispersal patterns and behaviour of North Sea cod (*Gadus morhua*) studied using electronic data storage tags. Hydrobiologia, **483**: 201–208. doi:10.1023/A:1021344015515.

Viterbi, A.J. 2006. A personal history of the Viterbi algorithm. IEEE Signal Process. Mag. **23**: 120–142. doi:10.1109/MSP.2006.1657823.

Welch, D.W., and Eveson, J.P. 1999. An assessment of light-based geoposition estimates from archival tags. Can. J. Fish. Aquat. Sci. **56**: 1317–1327. doi:10.1139/cjfas-56-7-1317.